FACTORS INFLUENCING MICRO SWEEP EFFICIENCY WHEN FLOODING A FORMATION WITH VISCOELASTIC POLYMER SOLUTIONS

Yikun Liu,[1] Huiying Zhong,[1] Xiaojuan Peng,[2] and Changliang Zhao[3]

A mathematical model is proposed for polymer solution flow in dead-end pores, which was studied using micro-seepage of polymer solutions as an example. The mathematical model, including a continuity equation, a momentum conservation equation, and an equation of state, was solved by the finite difference method. The stream function and velocity contours were determined. The micro sweep efficiency when flooding the formation was calculated based on the velocity contour. The influence of elasticity, flow velocity, and viscosity of the polymer solution on the micro sweep efficiency was evaluated. It is demonstrated that the viscosity and the injection rate have a lesser effect on micro sweep efficiency than the elasticity of the polymer solution.

Key words: *viscoelastic polymer solution, flooding sweep efficiency, velocity contour, polymer flooding.*

Polymer flooding has been successfully used as an enhanced oil recovery (EOR) method [1-3].

It was previously assumed that the mechanism for enhanced oil recovery with polymer flooding involves reducing the mobility ratio and increasing the macro sweep efficiency. However, recently it was observed that polymer solutions can significantly improve the micro sweep efficiency because of viscoelastic flow in a porous medium, which is significantly different from Newtonian flow [4-6].

---

[1]Key Laboratory of Enhanced Oil & Gas Recovery, Ministry of Education, Northeast Petroleum University (China). E-mail: zhhy987@126.com. [2]Oil Recovery Plant No. 1, Daqing Oilfield Company Limited (China). [3]Offshore Petroleum Development Company, Liaohe Oilfield Company (China). Translated from *Khimiya i Tekhnologiya Topliv i Masel*, No. 2, pp. 18 – 21, March– April, 2015.

A number of papers have been devoted to the influence of the viscoelastic properties of polymer solutions on oil displacement efficiency. Xia et al. [7] compared the displacement efficiency for a viscoelastic polymer solution with the displacement efficiency for a glycerin solution of the same viscosity. It is shown that polymer solutions are characterized by greater displacement efficiency. Yue et al. [8], based on results of a study of the flow characteristics of a polymer solution in dead-end pores, showed that the flow rate can be improved by increasing the viscosity of the polymer solution. The residual oil thus becomes recoverable oil [8]. However, the micro sweep efficiency is not only affected by the elasticity but also by the viscosity and flow velocity. In this paper, we have constructed a mathematical model of polymer solution flow in dead-end pores, and we have analyzed the factors influencing the micro sweep efficiency.

Governing equations. We considered the flow as two-dimensional isothermal steady flow. The model includes a continuity equation, a momentum conservation equation, and a constitutive equation (equation of state). The governing equations are dimensionless [9-11].
Continuity equation:

$$\frac{\partial u}{\partial x} + \frac{\partial u}{\partial y} = 0 \tag{1}$$

where u, v are the velocity components in the x and y directions respectively.
Momentum conservation equation:

$$\mathbf{Re}\left[\frac{\partial}{\partial x}(uu) + \frac{\partial}{\partial y}(uv)\right] = \frac{\partial \rho}{\partial x} + \frac{\partial T^{xx}}{\partial x} + \frac{\partial T^{xy}}{\partial y} \tag{2}$$

$$\mathbf{Re}\left[\frac{\partial}{\partial x}(vv) + \frac{\partial}{\partial y}(vu)\right] = \frac{\partial \rho}{\partial y} + \frac{\partial T^{xx}}{\partial x} + \frac{\partial T^{yy}}{\partial y} \tag{3}$$

where T^{xx}, T^{xy}, T^{yy} are the stresses in the corresponding directions; $Re = \rho UL/\mu$; U is the characteristic velocity (the average velocity at the inlet); ρ is the density of the polymer solution, kg/m^3; μ is the viscosity of the polymer solution, Pa·s; L is the characteristic length.
The rheological behavior of polymer solutions is determined mainly by the primary normal stress difference. The upper-convected Maxwell (UCM) equation corresponds to this property:

$$A_1\tau^{xx} + \mathbf{We}\left(u\frac{\partial \tau^{xx}}{\partial x} + v\frac{\partial \tau^{xx}}{\partial y}\right) = 2B\tau^{xy} + F_1 \tag{4}$$

$$A_2\tau^{xy} + \mathbf{We}\left(u\frac{\partial \tau^{xy}}{\partial x} + v\frac{\partial \tau^{xy}}{\partial y}\right) = C\tau^{xx} + B\tau^{yy} + F_2 \tag{5}$$

$$A_3 \tau^{yy} + \mathbf{We}\left(u\frac{\partial \tau^{yy}}{\partial x} + v\frac{\partial \tau^{yy}}{\partial y}\right) = C\tau^{xy} + F_3 \tag{6}$$

where

$$A_1 = 1 - 2\,\mathbf{We}\,\frac{\partial u}{\partial x}\;;\; A_2 = 1\;;\; A_3 = 1 - 2\,\mathbf{We}\,\frac{\partial v}{\partial y}\;;\; B = \mathbf{We}\,\frac{\partial u}{\partial y}\;;\; C = \mathbf{We}\,\frac{\partial v}{\partial x}$$

$$F_1 = 2\frac{\partial u}{\partial x}\left[2\left(\frac{\partial u}{\partial x}\right)^2 + 2\left(\frac{\partial v}{\partial y}\right)^2 + \left(\frac{\partial u}{\partial y} + \frac{\partial v}{\partial x}\right)^2\right]$$

$$F_2 = \left(\frac{\partial u}{\partial y} + \frac{\partial v}{\partial x}\right)\left[2\left(\frac{\partial u}{\partial x}\right)^2 + 2\left(\frac{\partial v}{\partial y}\right)^2 + \left(\frac{\partial u}{\partial y} + \frac{\partial v}{\partial x}\right)^2\right]$$

$$F_3 = 2\frac{\partial v}{\partial y}\left[2\left(\frac{\partial u}{\partial x}\right)^2 + 2\left(\frac{\partial v}{\partial y}\right)^2 + \left(\frac{\partial u}{\partial y} + \frac{\partial v}{\partial x}\right)^2\right]$$

In the equations given above, τ is the stress in the corresponding direction; $We = \lambda U/L$; λ is the relaxation time of the polymer solution, in seconds. The parameters L, U, T are dimensionless.

Numerical solution is made difficult due to the lack of a pressure equation. The term containing pressure does not have to be solved in velocity – stream function variables; the continuity equation can be solved automatically. The stream function and vorticity are defined by the equations:

$$u = \frac{\partial \psi}{\partial y}\;;\; v = \frac{\partial \psi}{\partial y} \tag{7}$$

$$\omega = \frac{\partial v}{\partial x} - \frac{\partial u}{\partial y} \tag{8}$$

where ω is the vorticity; ψ is the stream function.

These expressions were substituted into Eq. (3):

$$\omega = -\nabla^2 \psi \tag{9}$$

$$\frac{\partial^2 \omega}{\partial y^2} + \frac{\partial^2 \omega}{\partial x^2} + \mathbf{Re}\left(\frac{\partial \psi}{\partial x}\frac{\partial \omega}{\partial y} - \frac{\partial \psi}{\partial y}\frac{\partial \omega}{\partial x}\right) =$$

$$= \frac{\partial^2 T^{xx}}{\partial x \partial y} + \frac{\partial^2 T^{xy}}{\partial y^2} - \frac{\partial^2 T^{xy}}{\partial x^2} - \frac{\partial^2 T^{yy}}{\partial x \partial y} + \frac{\partial^3 y}{\partial x^3} - \frac{\partial^3 u}{\partial x^2 \partial y} + \frac{\partial^3 v}{\partial x \partial y^2} - \frac{\partial^3 u}{\partial y^3} \tag{10}$$
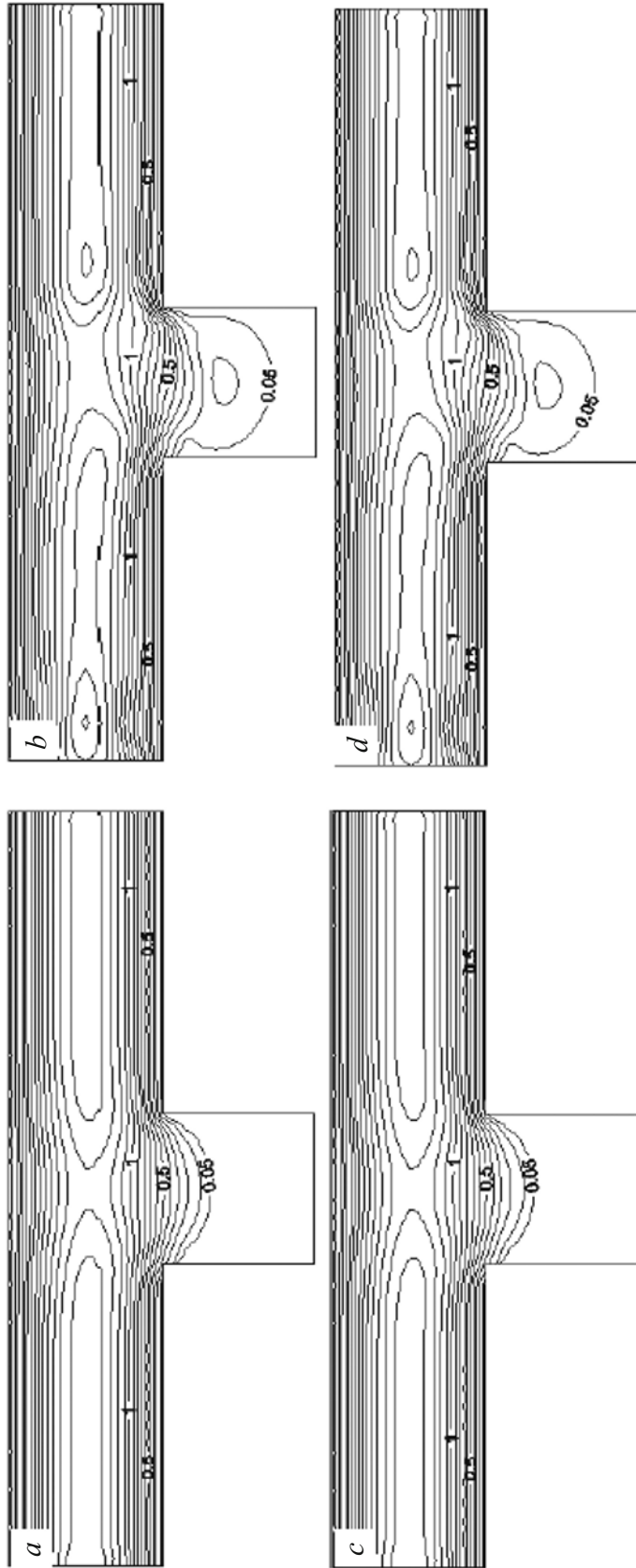
162

Fig. 1. Velocity contours: *a*) We = 0, Re = 5·10⁻⁵; *b*) We = 0.3, Re = 5·10⁻⁵; *c*) We = 0, Re = 0.1; *d*) We = 0.3, Re = 0.1.

Boundary conditions. For the dead-end model, the inlet conditions are: $u = 6(y - y^2)$, $v = 0$. The boundary conditions when parallel to the x axis are: $u = 0$, $v = 0$. The boundary conditions when parallel to the y axis are: $u = 0$, $v = 0$. The outlet conditions correspond to the Neumann boundary condition. The velocity gradient at the outlet is equal to zero, and so $u_{NI} = u_{NI-1}$.

Numerical simulation. A nonuniform grid was used for going to the difference equations from (4)-(6), (9), and (10). The stream function equation was solved by a central finite difference method. The left-hand and right-hand sides of the vorticity equation were transformed by a first-order upwind difference scheme and a central difference scheme. When $A_m \leq 0$ ($m = 1, 2, 3$), we use a downwind difference scheme; when $A_m \geq 0$, we use an upwind difference scheme.

$$\frac{\psi_{j+1,k} - 2\psi_{j,k} + \psi_{j-1,k}}{H_x^2} + \frac{\psi_{j+1,k} - 2\psi_{j,k} + \psi_{j-1,k}}{H_y^2} = -\omega_{j,k} \tag{11}$$

$$k_0\omega_{j,k} + k_1\omega_{j-1,k} + k_3\omega_{j,k+1} + k_4\omega_{j,k-1} = \frac{1}{4H_x H_y}\left(S_{j+1,k+1}^{xx} + S_{j-1,k+1}^{xx} + S_{j+1,k-1}^{xx} + S_{j-1,k-1}^{xx}\right) =$$

$$= \frac{1}{H_y^2}\left(S_{j,k+1}^{xy} - 2S_{j,k}^{xy} + S_{j,k-1}^{xy}\right) - \frac{1}{H_x^2}\left(S_{j+1,k}^{xy} - 2S_{j,k}^{xy} + S_{j-1,k}^{xy}\right) \tag{12}$$

where H_x and H_y are the mesh spacing in the x and y directions; for S, see (14).

$$k_0 = -\frac{2}{H_x^2} - \frac{2}{H_y^2} - 2\left(|f_1| + |f_2|\right); \quad k_2 = \frac{1}{H_x^2} + |f_2| - f_2; \quad k_4 = \frac{1}{H_y^2} + |f_1| - f_1$$

$$f_1 = \frac{b_1}{2H_y}; f_2 = \frac{b_2}{2H_x}$$

$$b_1 = \mathbf{Re}\frac{\psi_{j+1,k} - \psi_{j-1,k}}{2H_x}; \quad b_2 = -\mathbf{Re}\frac{\psi_{j,k+1} - \psi_{j,k-1}}{2H_y}$$

$$k_0^{A_1}T_{j,k}^{xx} - k_1^{A_1}T_{j+1,k}^{xx} - k_2^{A_1}T_{j-1,k}^{xx} - k_3^{A_1}T_{j,k+1}^{xx} - k_4^{A_1}T_{j,k-1}^{xx} = \left(2B_{j,k}T_{j,k}^{xy} + F_{1j,k}\right)\mathbf{sgn}(A_1)$$

$$k_0^{A_2}T_{j,k}^{xy} - k_1^{A_2}T_{j+1,k}^{xy} - k_2^{A_2}T_{j-1,k}^{xy} - k_3^{A_2}T_{j,k+1}^{xy} - k_4^{A_2}T_{j,k-1}^{xy} = \left(C_{j,k}T_{j,k}^{xx} + B_{j,k}T_{j,k}^{xy} + F_{2j,k}\right)\mathbf{sgn}(A_2)$$

$$k_0^{A_3}T_{j,k}^{yy} - k_1^{A_3}T_{j+1,k}^{yy} - k_2^{A_3}T_{j-1,k}^{yy} - k_3^{A_3}T_{j,k+1}^{yy} - k_4^{A_3}T_{j,k-1}^{yy} = \left(2C_{j,k}T_{j,k}^{xy} + F_{3j,k}\right)\mathbf{sgn}(A_3) \tag{13}$$

In Eq. (13),

$$k_1 = \left|B_1^{A_m}\right| - B_1^{A_m}; \quad k_2 = \left|B_1^{A_m}\right| + B_1^{A_m}; \quad k_3 = \left|B_2^{A_m}\right| - B_2^{A_m}; \quad k_4 = \left|B_2^{A_m}\right| + B_2^{A_m}$$

The coefficients A, B, C, and F are calculated by a central difference scheme.

The additional stress tensor due to non-Newtonian flow is expressed by the equation:

$$\left. \begin{array}{l} S_{j,k}^{xx} = T_{j,k}^{xx} - F_{1j,k} \\ S_{j,k}^{xy} = T_{j,k}^{xy} - F_{2j,k} \\ S_{j,k}^{yy} = T_{j,k}^{yy} - F_{3j,k} \end{array} \right\} \qquad (14)$$

The nonlinear equations were solved by relaxation methods. The inner iteration of the linear differential equations was solved by the Gauss – Seidel iteration method. The external iteration, concluding with the equations and boundary conditions, was solved by the under-relaxation method.

Analysis of hydrodynamic characteristics. The stream functions, the velocity, and the stress were calculated according to the simulation model described above. We compared the velocity contours for the different conditions (Fig. 1). As we see, the sweep area, bounded by the 0.05 line, increases as the Weber number (We) increases, i.e., as the elasticity of the polymer solution increases. We also see that the velocity contour changes only very slightly as the Reynolds number (Re) changes.

Factors influencing micro sweep efficiency. The micro sweep efficiency was calculated based on the velocity contour:

$$\eta = \frac{A_1}{A_1 + A_2} 100\%$$

In this equation, A_1 and A_2 are defined as shown in Fig. 2.

The elasticity of the polymer solutions was determined from the relaxation time. A longer relaxation time means higher elasticity of the solution. In the dimensionless calculations, the Weber number is proportional to the relaxation time, i.e., a higher We means higher elasticity. Figure 3 shows the results of calculating the micro sweep efficiency for the same values of the Reynolds number (10^{-5}) but different values of the Weber number. As we see, the micro sweep efficiency increases as the Weber number increases for We above 0.15.
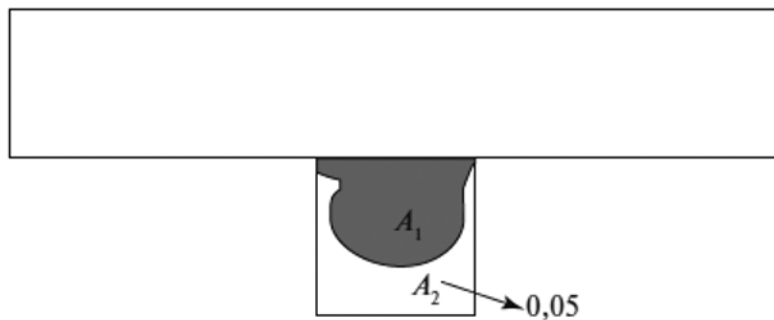

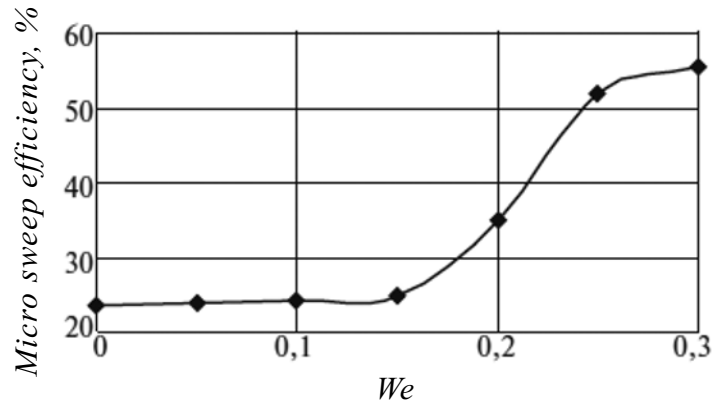Fig. 2. Schematic diagram for determining the micro sweep efficiency.

Fig. 3. Micro sweep efficiency vs. elasticity of the polymer solution.
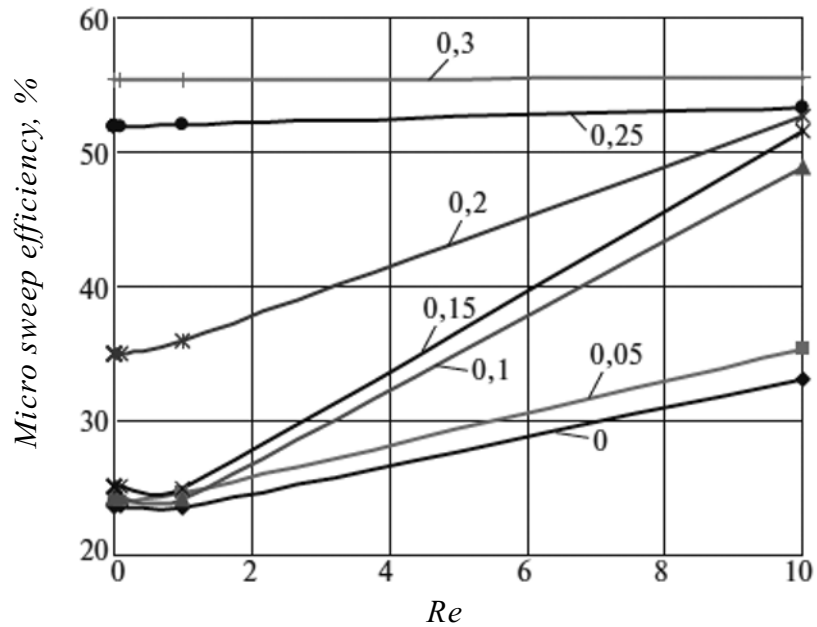

Fig. 4. Micro sweep efficiency vs. Reynolds number and Weber number (see numbers on curves).

The dimensionless quantity Re is inversely proportional to viscosity. Figure 4 shows the change in the micro sweep efficiency as the Reynolds number is varied. As we see, the micro sweep efficiency increases as the Reynolds number increases, i.e., as the viscosity decreases. With a decrease in the viscosity of the solution, the resistance to flow decreases and so the micro sweep efficiency increases for dead-end pores. From Fig. 4, we also see that the micro sweep efficiency does not depend much on viscosity for the low Reynolds number values characteristic under reservoir conditions.

The dimensionless quantity Re is directly proportional to the flow velocity of the polymer solution. From Fig. 4, we see that the micro sweep efficiency increases with the Reynolds number and consequently with the flow velocity. However, under reservoir conditions, the Reynolds number varies in the range from 10^{-5} to 1. In this range, the Re value has practically no effect on the micro sweep efficiency.

Therefore the elasticity of the polymer solution is the major factor influencing micro sweep efficiency.

REFERENCES

1. P. Corlay and E. Delamaide, *Journal of Petroleum Technology*, No. 3, 198-199 (1996).
2. G. J. Wang, O. Y. Jian, and X. L. Yi, *Chemistry and Technology of Fuels and Oils*, No. 4, 263-267 (2011).
3. R. S. Seright, *SPE Reservoir Evaluation & Engineering*, No. 4, 730-740 (2010).
4. J. W. Zhang, *Petrochemical Industry of Inner Mongolia*, No. 3, 28-30 (2013).
5. T. S. Urbissinova, J. J. Trivedi, and E. Kuru, *Journal of Canadian Petroleum Technology*, No. 12, 49-56 (2010).
6. T. Clemens, K. Tsikouris, M. Buchgraber et al., in: *SPE Improved Oil Recovery Symposium, 14-18 April 2012, Tulsa USA* (2012); SPE 154169.
7. H. F. Xia, D. M. Wang, Z. C. Liu et al., *Acta Petrolei Sinica*, No. 4, 60-65 (2001).
8. X. A. Yue, L. J. Zhang, Z. C. Liu et al., *Petroleum Geology and Recovery Efficiency*, No. 3, 4-6 (2002).
9. H. J. Yin, D. M. Wang, H. Y. Zhong et al., in: *SPE EOR Conference at Oil and Gas West Asia, 16-18 April 2012, Muscat, Oman* (2012); SPE 154640.
10. H. Y. Zhong, Z. Tian, and H. J. Yin, *Chemistry and Technology of Fuels and Oils*, No. 5, 393-402 (2012).
11. H. Y. Zhong and H. J. Yin, in: *International Conference on Energy and Environment Technology, 16-18 October 2009, Guilin, China*, IEEE Computer Society (2009); pp. 427-430.